Iron/Photosensitizer Hybrid System Enables the Synthesis of Polyaryl-Substituted Azafluoranthenes

Yoshimi Kato,[1] Tatsuhiko Yoshino,[1,2] Min Gao,[3] Jun-ya Hasegawa,[3] Masahiro Kojima,[1]* and Shigeki Matsunaga.[1,2]*

[1] Faculty of Pharmaceutical Sciences, Hokkaido University, Sapporo 060-0812, Japan.

[2] Global Station for Biosurfaces and Drug Discovery, Hokkaido University, Sapporo 060-0812, Japan

[3] Institute for Catalysis, Hokkaido University, Sapporo 001-0021, Japan.

ABSTRACT: Photosensitization of organometallics is a privileged strategy that enables challenging transformations in transition metal catalysis. However, the usefulness of such photocatalyst-induced energy transfer has remained opaque in iron-catalyzed reactions despite the intriguing prospects of iron catalysis in synthetic chemistry. Herein, we demonstrate the use of iron/photosensitizer-cocatalyzed cycloaddition to synthesize polyarylpyridines and azafluoranthenes, which have been scarcely accessible using the established iron-catalyzed protocols. Mechanistic studies indicate that triplet energy transfer from the photocatalyst to a ferracyclic intermediate facilitates the thermally demanding nitrile insertion and accounts for the distinct reactivity of the hybrid system. This study thus provides the first demonstration of the role of photosensitization in overcoming the limitations of iron catalysis.

INTRODUCTION

Photochemistry plays indispensable roles in molecular sciences, as it enables reactions that are not feasible using the reactants in their ground state.[1] While direct photoexcitation is a straightforward approach to access excited states, its efficiency depends on the various absorption spectra of the compounds, which occasionally leads to limited generality in synthetic applications. On the other hand, photosensitization using photocatalysts provides a more general strategy to achieve excited state reactivities.[2] In this regard, the photosensitization of organometallic intermediates in a catalytic cycle has recently been recognized as a privileged strategy for the development of new reactions (**Figure 1A**, top). Nevertheless, successful merger of the transition metal catalysis and photosensitizer-induced energy transfer (EnT) has so far been limited to reactions via organonickel,[3] organopalladium,[4] or organogold[5] intermediates, and application of the photosensitization strategy to other transition metal catalysis remains elusive.[6,7]

In this context, the photosensitization of organoiron species deserves particular attention, considering the sustainability and unique reactivity of iron catalysts.[8] However, few such attempts have been reported in synthetic chemistry, despite the well-known roles of organoiron compounds in catalytic bond-forming reactions (**Figure 1A**, bottom). Notably, Chakraborty and Jacobi von Wangelin reported an iron/9,10-diphenylanthracene(DPA)-cocatalyzed trimerization of alkynes in which dissociation of the iron catalyst and the product is promoted by photosensitization (**Figure 1B**).[9] Nonetheless, the substrate scope of this reaction does not exceed the scope of thermal iron catalysis,[10] and the unique synthetic advantages of combining iron catalysis and photocatalysis have yet to be elucidated.[11]

Transition-metal-catalyzed [2+2+2] cycloaddition of diynes and nitriles, by which pyridines are constructed in one step, is an atom-economical method to access natural products and π-extended molecules.[12] In thermal systems, iron-catalyzed [2+2+2] cycloaddition has been achieved using low-valent iron complexes[13] or iron/additive systems in which low-valent iron species are generated *in situ*.[10,14] However, applicable diynes have been limited to alkyl-substituted ones, and there are no reports using aryl-substituted diynes to enable the synthesis of polyarylpyridines, which are common motifs in functional molecules (**Figure 1C**). As a result of our effort to overcome the limitations of iron catalysis using photosensitization, herein we report an iron/photosensitizer-cocatalyzed [2+2+2] cycloaddition using aryl-substituted diynes and nitriles, which enables the chemoselective synthesis of polyarylpyridines (**Figure 1D**). In addition, modular synthesis of polyaryl-substituted azafluoranthenes, which are promising scaffolds for organic electro-luminescence materials, was also realized. Mechanistic experiments, DFT, and SAC-CI calculations suggest that energy transfer from the photosensitizer to an organoiron intermediate is likely to be responsible for the distinct reactivity of the developed catalytic system.

RESULTS AND DISCUSSION

Studies of reaction conditions and substrate scope. After several trials, iron-catalyzed [2+2+2] cycloaddition of aryl-substituted diyne **1a** with benzonitrile **2a** proceeded in high yield in the presence of FeI_2 (99.99% metals basis), dppp, $[Ir(dF(CF_3)ppy)_2(dtbbpy)]PF_6$ and triethylamine (an electron donor for generating a low-valent iron catalyst *in situ*) under blue LED irradiation (Table 1, entry 1). The high purity of FeI_2 indicates that the effect of the contamination of other transition metals is negligible. When $FeBr_2$ (entry 2) and $FeCl_2$ (entry 3) were used instead of FeI_2, the yields decreased in the order FeI_2 > $FeBr_2$ > $FeCl_2$. $Fe(OAc)_2$, $Fe(acac)_2$ and $Fe(BF_4)\cdot nH_2O$ (entries 4–6) did not afford the desired product **4aa**, suggesting that halide is crucial for this reaction to proceed.[15] Evaluation of other ligands revealed that dppp is specifically suitable for

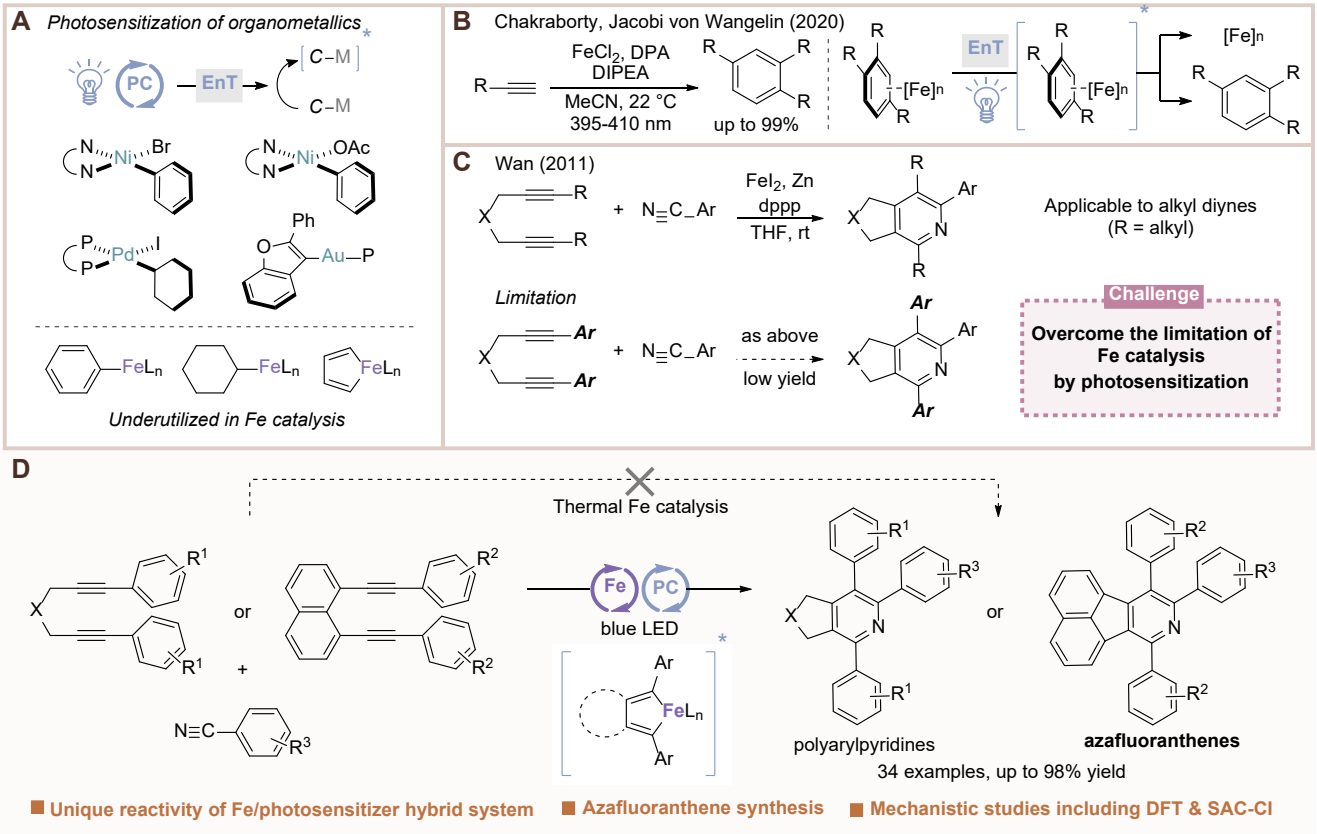

Figure 1. (A) Photosensitization as an enabling strategy in transition metal catalysis. (B) Iron/photoredox catalysis for the trimerization of alkynes. (C) Iron-catalyzed [2+2+2] cycloaddition using diynes and nitriles under thermal conditions. (D) This work: Synthesis of polyarylpyridines and azafluoranthenes using an iron/photosensitizer hybrid system.

Table 1. Evaluation of reaction conditions for [2+2+2] cycloaddition under the iron/photosensitizer hybrid system.[a]

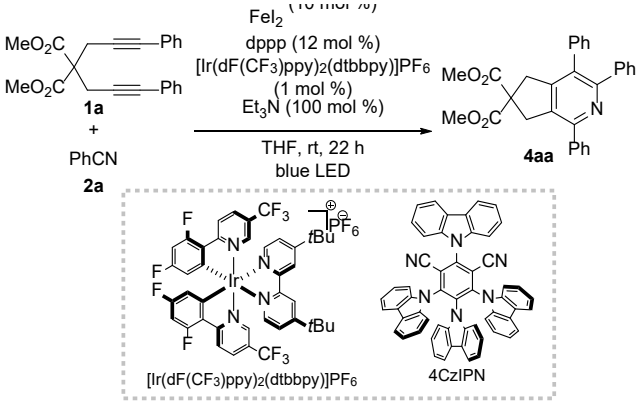

Entry	Variation from above	Yield[b] (%)
1	none	85[c]
2	$FeBr_2$ instead of FeI_2	57
3	$FeCl_2$ instead of FeI_2	26
4	$Fe(OAc)_2$ instead of FeI_2	0
5	$Fe(acac)_2$ instead of FeI_2	0
6	$Fe(BF_4)_2 \cdot nH_2O$ instead of FeI_2	0
7	dppe instead of dppp	16
8	dppb instead of dppp	0
9	dppbz instead of dppp	9
10	*cis*-dppen instead of dppp	60
11	PPh_3 (12 mol%) instead of dppp	0
12	1,10-phenanthroline instead of dppp	9
13	dtbbpy instead of dppp	0
14	4CzIPN instead of $[Ir(dF(CF_3)ppy)_2(dtbbpy)]PF_6$	86[c]
15	without $[Ir(dF(CF_3)ppy)_2(dtbbpy)]PF_6$	0

[a]Reaction conditions: **1a** (0.10 mmol), **2a** (0.50 mmol), FeI_2 (99.99% metals basis, 10 μmol, 10 mol%), dppp (12 μmol, 12 mol%), photocatalyst (1.0 μmol, 1 mol%), Et_3N (0.10 mmol, 100 mol%) in THF (0.5 mL) at room temperature for 22 hours under blue LED irradiation. [b]^1H NMR yield. [c]Isolated yield. For details, see Supporting Information.

this reaction, while *cis*-dppen manifested certain reactivity (entries 7–13). The origin of the beneficial effect of dppp is unclear, but it is occasionally identified to be suitable for reactions catalyzed by low-valent first-row metals.[16] When 4CzIPN was used instead of $[Ir(dF(CF_3)ppy)_2(dtbbpy)]PF_6$, the reaction proceeded smoothly (entry 14), suggesting that the iron/photosensitizer hybrid catalysis is also operative under noble-metal-free conditions. The desired product was not obtained in the absence of the photocatalyst (entry 15).

The scope of the iron/photosensitizer-catalyzed cycloaddition in terms of diynes **1** and nitriles **2** is summarized in **Scheme 1**. Nitriles possessing various aromatic rings or alkyl groups underwent the desired cycloaddition (**4aa**–**4am**). It is noteworthy that synthesis of **4aa** can be performed on a 1 gram

scale in 80% yield. The cycloaddition of various aryl-substituted diynes **1** also proceeded smoothly (**4ba**, **4ca**, **4db**, **4ea**). Different tethers and alkyl substituents were tolerated in the pyridine synthesis (**4fa**–**4ja**). The amount of the iron catalyst could be decreased to 5 mol% and the amount of nitrile to 2.5 equivalents when methyl-substituted diynes were used (**4ga**–**4ia**). The catalyst loading of iron could be decreased to 1 mol% and photocatalyst to 0.1 mol% by modifying the reaction conditions (**4ha**).

Scheme 1. Substrate scope of polyaryl-substituted pyridines[a]

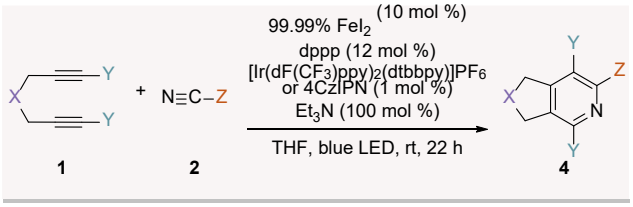

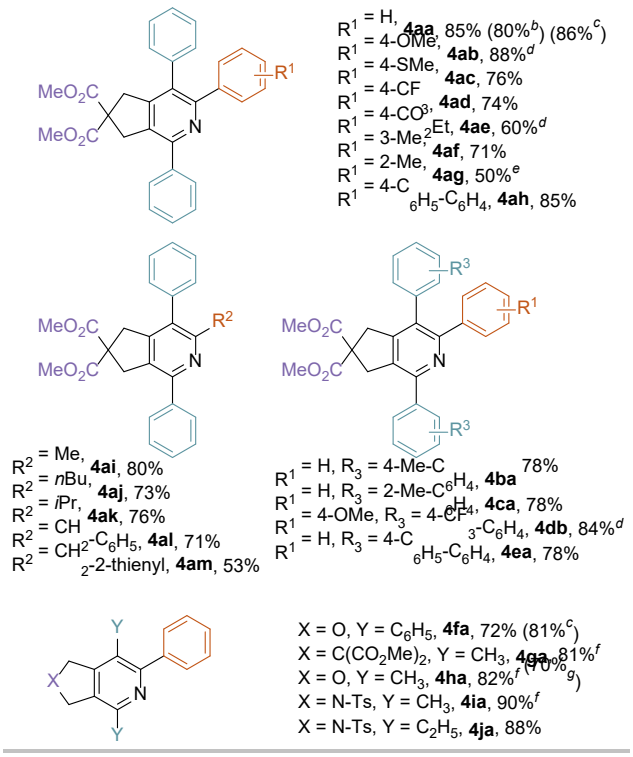

[a]Reaction conditions: **1** (0.30 mmol), **2** (1.5 mmol), FeI_2 (99.99%, trace metal basis, 30 µmol, 10 mol%), dppp (36 µmol, 12 mol%), $[Ir(dF(CF_3)ppy)_2(dtbbpy)]PF_6$ (3.0 µmol, 1.0 mol%), Et_3N (0.30 mmol, 100 mol%), THF (1.5 mL) at room temperature for 22 hours under blue LED irradiation. Isolated yields. [b]Using **1a** (1.0 g, 2.8 mmol) and blue LED panel × 2 (see Supporting Information for the detailed reaction setup) under temperature control for 72 hours. [c]4CzIPN (1.0 mol%) was used instead of $[Ir(dF(CF_3)ppy)_2(dtbbpy)]PF_6$. [d]**2** (2.4 mmol). [e]**2** (3.0 mmol). [f]FeI_2 (15 µmol, 5.0 mol%), dppp (18 µmol, 6.0 mol%), $[Ir(dF(CF_3)ppy)_2(dtbbpy)]PF_6$ (1.5 µmol, 0.50 mol%), **2** (0.75 mmol). [g]FeI_2 (3.0 µmol, 1.0 mol%), dppp (3.6 µmol, 1.2 mol%), $[Ir(dF(CF_3)ppy)_2(dtbbpy)]PF_6$ (0.30 µmol, 0.10 mol%), Et_3N (0.15 mmol, 50 mol%), **2** (0.75 mmol), THF (300 µL).

Azafluoranthenes, an azaheterocycle possessing a 6/6/5/6-fused 16π-antiaromatic system, represent an actively studied structural motif in electroluminescent materials.[17] However, the known preparative methods for azafluoranthenes suffer from high temperature requirements (250–300 °C),[17a] limited generality[17b,17c] or the use of isonitriles.[17d] Gratifyingly, by applying the iron/photosensitizer hybrid system to the [2+2+2] cycloaddition of diyne **3** and nitrile **2**, a variety of polyaryl-substituted azafluoranthenes were prepared in a modular manner (**Scheme 2**). The cycloaddition of 1,8-bis(phenylethynyl)naphthalene **3a** and **2a** afforded the corresponding azafluoranthene nearly quantitatively (**5aa**, 97%). In addition, **5aa** can be obtained in 73% yield on a 1.0 mmol scale. The cycloaddition also proceeded in synthetically useful yield under noble-metal-free conditions using 4CzIPN as the organic photosensitizer (**5aa**, 71%). Other nitriles provided the desired products in 34–98% yield (**5aa**–**5ae**, **5an**, **5ah**, **5ai**). The structure of azafluoranthene **5ac** was unambiguously confirmed via single-crystal X-ray diffraction analysis. Diynes with different electronic character afforded the desired products in 46–98% yield (**5ba**, **5ca**, **5cb**, **5da**).[18,19] In addition, **5da** was also obtained using iron/4CzIPN hybrid system in 69% yield.[20,21]

Scheme 2. Substrate scope of polyaryl-substituted azafluoranthenes[a]

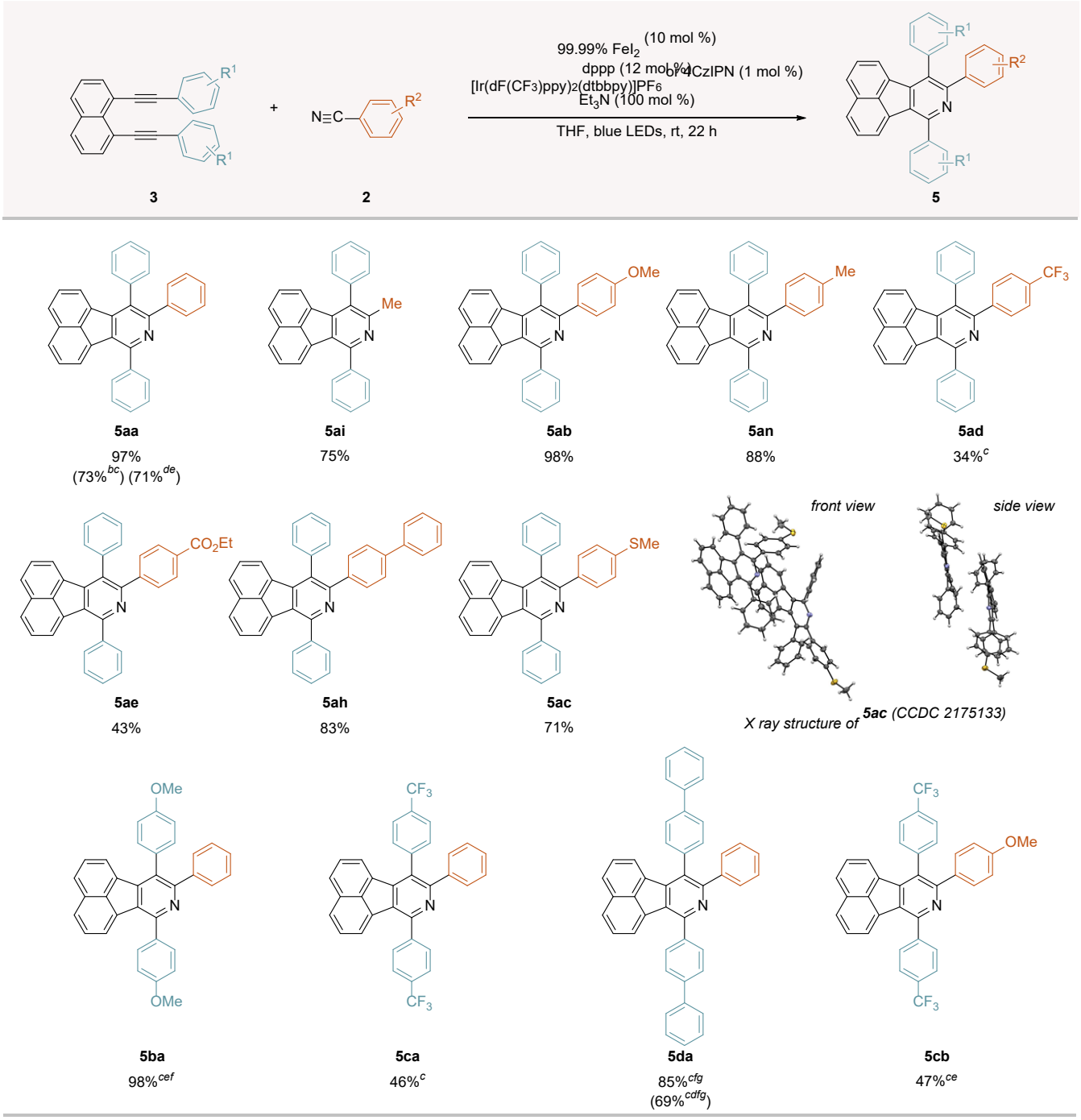

[a]Reaction conditions: **3** (0.30 mmol), **2** (3.0 mmol), FeI_2 (99.99%, trace metal basis, 30 μmol, 10 mol%), dppp (36 μmol, 12 mol%), $[Ir(dF(CF_3)ppy)_2(dtbbpy)]PF_6$ (3.0 μmol, 1.0 mol%), Et_3N (0.30 mmol, 100 mol%), THF (1.5 mL) at room temperature for 22 hours under blue LED irradiation. Isolated yields. [b]Using **3a** (1.0 mmol) for 72 hours. [c]Blue LED panel × 2 (see Supporting Information for the detailed reaction setup) under temperature control. [d]4CzIPN was used instead of $[Ir(dF(CF_3)ppy)_2(dtbbpy)]PF_6$. [e]0.20 mmol scale. [f]0.05 M. [g]0.10 mmol scale.

Comparison with thermal iron catalysis. The difference between the developed method and the previous iron-catalyzed [2+2+2] cycloaddition is summarized in **Scheme 3**. When **1f** and **3a** were subjected to Chakraborty and Jacobi von Wangelin's conditions,[9] the corresponding pyridine was not observed (**Scheme 3A, (i)(ii)**). Under Wan's conditions,[14a] the yield of pyridine was very low when **1f** or **3a** was used (**Scheme 3A, (iii)(iv)**). These results suggest that our iron/photosensitizer hybrid catalysis is uniquely suitable for polyarylpyridine synthesis compared to known iron catalysis.

Mechanistic studies. To gain insight into the unique reactivity of this reaction system, we performed two experiments: (1) light irradiation to Wan's conditions and (2) light irradiation to Wan's conditions in the presence of the photocatalyst (**Scheme 3B**). In case (1), the yield of **4fa** increased slightly (**Scheme 3B, (v)**, 33%) compared to that

Scheme 3. Comparison experiments with other conditions and evaluation of the light effect.

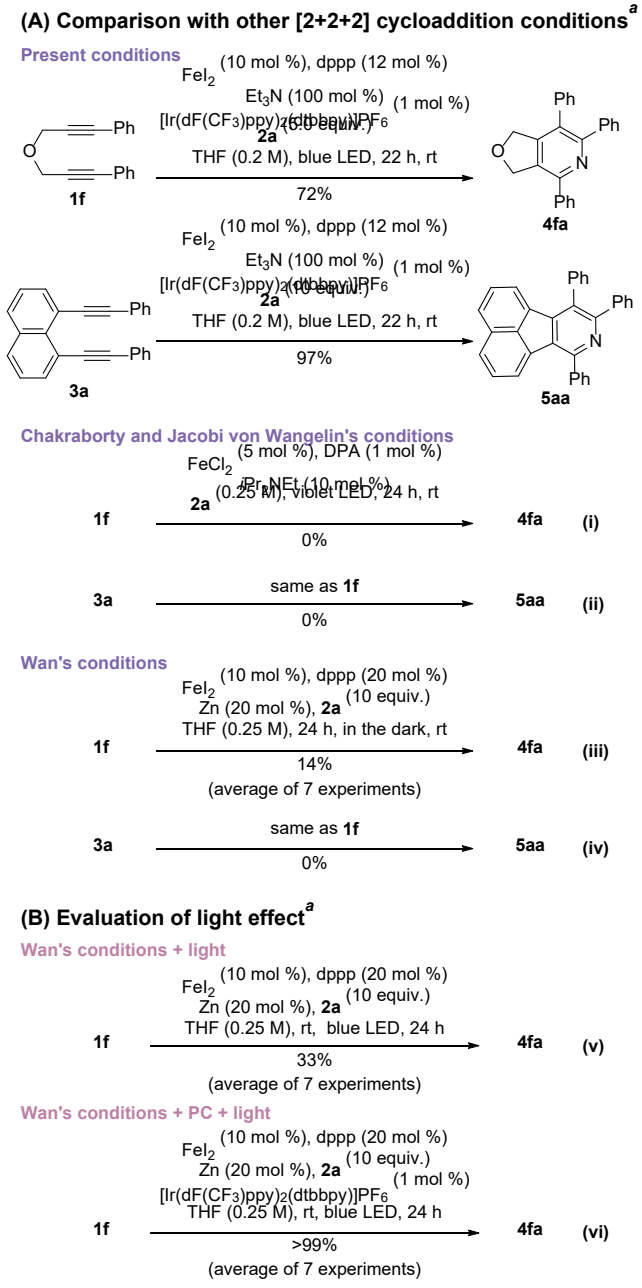

[a]See Supporting Information for details.

under the original conditions (**Scheme 3A, (iii)**, 14%),[22,23] suggesting an inefficient yet certain acceleration of the cycloaddition via the direct photoexcitation of an iron complex[24] generated *in situ*. In case (2), the reactivity increased dramatically, and **4fa** was obtained in >99% yield (**Scheme 3B, (vi)**). These results indicate that photoinduced energy transfer to a catalytic intermediate, rather than photoredox-induced electron transfer, is more likely to be responsible for accelerating the challenging cycloaddition toward polyarylpyridines.

To get insight of the catalytically active iron species, we conducted the cyclic voltammetry studies (**Figure 2**). The mixture of FeI_2 and dppp (molar ratio = 1:1.05) shows the Fe-centered reduction at –1.371 V vs. SCE (Fe^{II}/Fe^{I}) and at –1.869 V (Fe^{I}/Fe^{0}) (**Figure 2**, a). When the mixture of FeI_2, dppp and diyne **1a** (molar ratio = 1:1.05:10) were subjected to analysis, the Fe-centered reduction at –1.365 V (Fe^{II}/Fe^{I}) and –1.877 V (Fe^{I}/Fe^{0}) were observed (**Figure 2**, b). These results and the reduction potential of $[Ir(dF(CF_3)ppy)_2(dtbbpy)]PF_6$ ($E_{red}(Ir^{III}/Ir^{II})$ = –1.37 V vs. SCE) suggest that the catalytically active iron species is likely to be Fe^{I} and the reduction potential of iron was not affected in the presence of the diyne.

Figure 2. Cyclic voltammogram of Fe(dppp)I_2 in the absence or presence of 1a.[a]

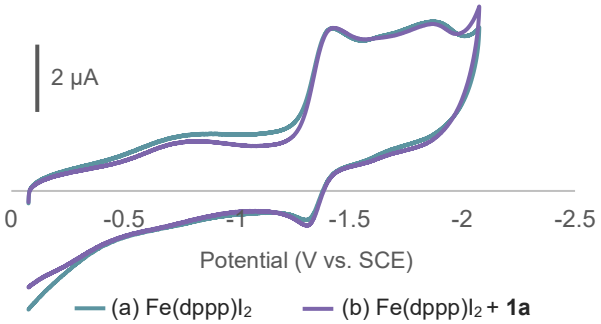

[a]See Supporting Information for details.

Next, we performed DFT calculations and obtained the energy diagrams of the iron-catalyzed [2+2+2] cycloaddition (**Scheme 4a**).[25] Based on the indispensability of halide anions (**Table 1**), propensity of dppp to form a 1:1 adduct with Fe(II) halide in the presence of THF,[26] and the results of the electrochemical study (**Figure 2**), the iodide-ligated Fe(I) diphenylphosphinopropane complex, which should be readily generated *in situ* by reduction of Fe(dppp)I_2, was employed as the catalyst in the theoretical study. In both the doublet and quartet states, the insertion of nitrile into the five-membered ferracycle intermediate was identified as the turnover-limiting step. The energy barrier of the insertion in quartet state was too high (quartet **INT1'** to quartet **TS2**: 40.3 kcal/mol) for the reaction to proceed at room temperature. In case spin crossover occurs at this step, the energy barrier is still high (quartet **INT1'** to doublet **TS2**: 22.8 kcal/mol), which is consistent with the experimental result that only 14% of **4fa** was obtained under thermal conditions. We surmise that the photoexcitation of the quartet **INT1'** accounts for the distinct reactivity of the iron/photosensitizer hybrid system. In the presence of the photocatalyst, energy transfer from the excited photocatalyst to quartet **INT1'** brings the organoiron intermediate into its doublet excited state $\mathbf{D_n}$. Then, spin-allowed decay of $\mathbf{D_n}$ to doublet **INT1'** allows the nitrile insertion to proceed through the doublet energy surface (doublet **INT1'** to doublet **TS2**: 8.6 kcal/mol).

The validity of this mechanistic hypothesis was more accurately elucidated by the SAC-CI method[27] (**Scheme 4b**). The excited states of the quartet **INT1'** ($\mathbf{Q_0}$) were calculated, and three doublet excited states ($\mathbf{D_0}$, $\mathbf{D_1}$, $\mathbf{D_2}$) and one quartet excited state ($\mathbf{Q_1}$) were identified. The three doublet excited states were respectively at 27.5, 28.5, and 36.8 kcal/mol with respect to the ground state $\mathbf{Q_0}$ at –11.8 kcal/mol. The excitation energy to $\mathbf{D_0}$, $\mathbf{D_1}$, and $\mathbf{D_2}$ were, therefore, 39.3, 40.3, and 48.6 kcal/mol, respectively. Thus, they are within an accessible range by photosensitization of $\mathbf{Q_0}$ by $[Ir(dF(CF_3)ppy)_2(dtbbpy)]PF_6$ ($E(T_1)$ = 61.8 kcal/mol:[2a] reachable up to 50.0 kcal/mol in relative energy) or by 4CzIPN

Scheme 4. Rationale of the unique reactivity of the iron/photosensitizer-catalyzed [2+2+2] cycloaddition.

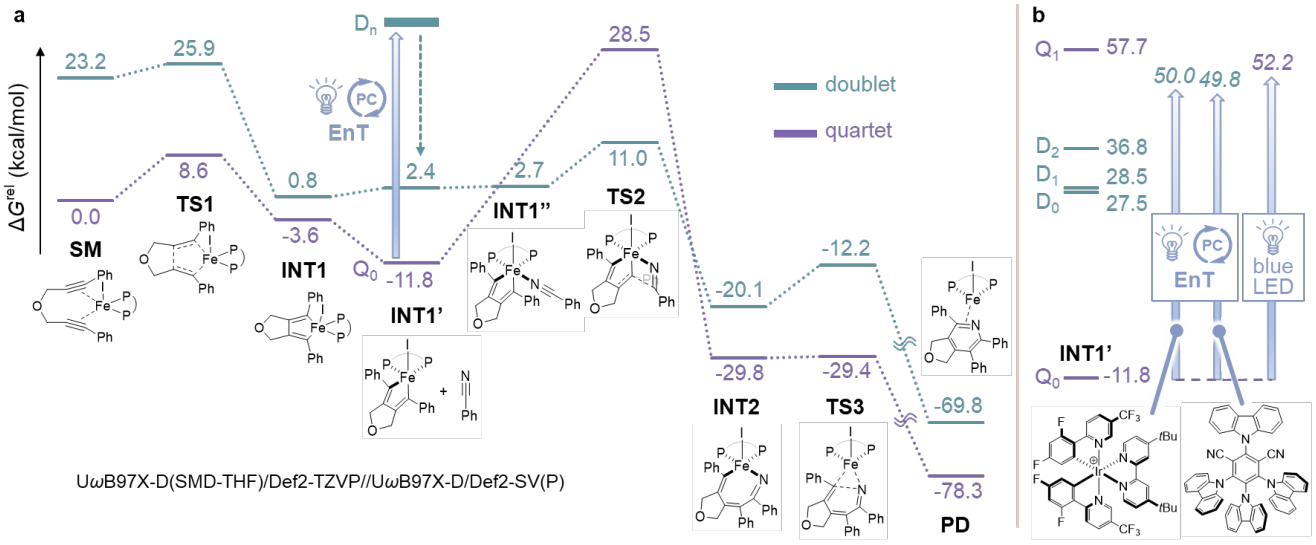

a) Computed energy diagrams of the cycloaddition using DFT. b) Relative energies of the excited states of **INT1'** calculated using the SAC-CI method. The energy of the quartet ground state $\mathbf{Q_0}$ is equalized to that of **INT1'** (–11.8 kcal/mol) to facilitate interpretation.

($E(T_1)$ = 61.6 kcal/mol: reachable up to 49.8 kcal/mol).[28] On the other hand, spin-allowed direct photoexcitation of $\mathbf{Q_0}$ to $\mathbf{Q_1}$ in the absence of a photosensitizer requires an energy as large as 69.5 kcal/mol. This value is larger than that available from the peak intensity of the blue LED (447 nm: 64.0 kcal/mol; reachable up to 52.2 kcal/mol), which may account for the limited efficiency of the cycloaddition under blue LED irradiation in the absence of the photocatalyst (**Scheme 3B, (v)**).

To elucidate the feasibility of the mechanism proposed in **Scheme 4**, in which one photon is required per each catalytic turnover, a couple of photochemical studies were conducted. First, quantum yield (Φ) of the cycloaddition toward **4fa** was measured (**Scheme 5A**) since the theoretical limit of Φ is 1 if the mechanism in **Scheme 4** is mainly responsible for the product formation. Thus, Φ of the overall transformation was determined to be 7%.[29] Second, light/dark experiment was conducted (**Scheme 5B**). In entry 1, the reaction mixture for the iron/photosensitizer-catalyzed [2+2+2] cycloaddition was irradiated for 3 hours and was worked up immediately. In entry 2, the reaction mixture was irradiated for 3 hours and then was stirred in the dark for the following 19 hours. Thus, **4fa** was obtained in 47% yield in entry 1 and in 45% yield in entry 2.[30] The small quantum yield of the reaction (Φ < 1) and the minute difference of the yield of two trials in **Scheme 5** suggest that dark catalytic turnover of photochemically generated species may not play a substantial role in the iron/photosensitizer-catalyzed cycloaddition. These observations agree with the proposed mechanism in **Scheme 4** which demands one photon for the photosensitization of **INT1'** in each catalytic cycle.

Scheme 5. Photochemical experiments toward mechanistic elucidation.[a]

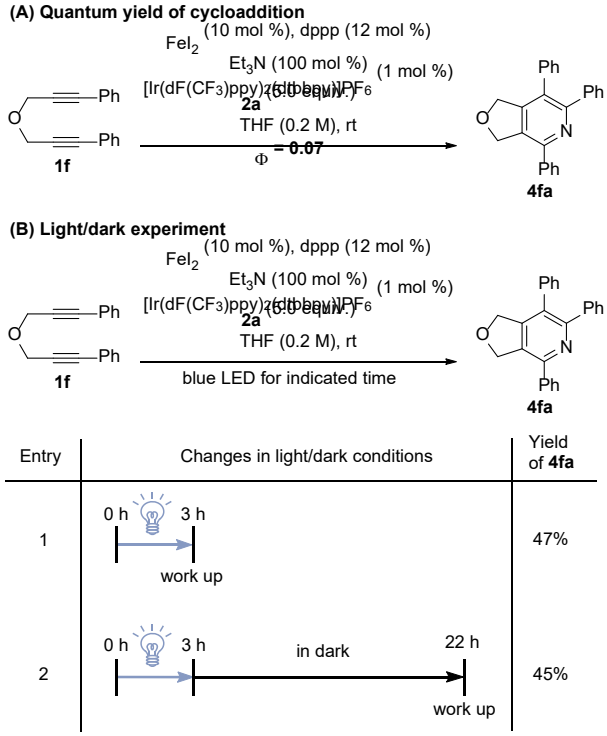

[a]See Supporting Information for experimental details.

CONCLUSIONS

In conclusion, we have developed an iron/photosensitizer-hybrid system that enables the hitherto-challenging iron-catalyzed [2+2+2] cycloaddition of diynes and nitriles toward the synthesis of polyarylpyridines. The unique reactivity of the developed method is highlighted by the modular syntheses of azafluoranthenes under mild and operationally benign conditions. Since the cycloaddition proceeds in only low yield under the reported iron-catalyzed protocol, our study clarified the potential of the iron/photocatalyst dual system to overcome the limitation of thermal iron catalysis. Experimental results and quantum chemical calculations suggest that

photosensitization of an organoiron intermediate is responsible for facilitating the thermally sluggish step in the catalytic cycle. The applicability of iron/photosensitizer dual catalysis in other modes of iron-catalysis is under investigation in our group.

ASSOCIATED CONTENT

Supporting Information.

The following files are available free of charge at https://pubs.acs.org.

Experimental procedures, characterization of the synthesized compounds, details of quantum chemical calculations, and NMR spectra (PDF). X-ray crystallographic data for the determination of the structure of **5ac** (CIF). These materials are available free of charge via the Internet at http://pubs.acs.org.

AUTHOR INFORMATION

Corresponding Author

Masahiro Kojima – Faculty of Pharmaceutical Sciences, Hokkaido University, Sapporo 060-0812, Japan; orcid.org/0000-0002-4619-2621; Email: m-kojima@pharm.hokudai.ac.jp

Shigeki Matsunaga – Faculty of Pharmaceutical Sciences, Hokkaido University, Sapporo 060-0812, Japan; Global Station for Biosurfaces and Drug Discovery, Hokkaido University, Sapporo 060-0812, Japan; orcid.org/0000-0003-4136-3548; Email: smatsuna@pharm.hokudai.ac.jp

Authors

Yoshimi Kato – Faculty of Pharmaceutical Sciences, Hokkaido University, Sapporo 060-0812, Japan.

Tatsuhiko Yoshino – Faculty of Pharmaceutical Sciences, Hokkaido University, Sapporo 060-0812, Japan; Global Station for Biosurfaces and Drug Discovery, Hokkaido University, Sapporo 060-0812, Japan; orcid.org/0000-0001-9441-9272.

Min Gao – Institute for Catalysis, Hokkaido University, Sapporo 001-0021, Japan; Present Address: Institute for Chemical Reaction Design and Discovery (WPI-ICReDD), Hokkaido University, Sapporo 001-0021, Japan; orcid.org/0000-0002-7263-1157.

Jun-ya Hasegawa –Institute for Catalysis, Hokkaido University, Sapporo 001-0021, Japan; orcid.org/0000-0002-9700-3309.

Notes

The authors declare no competing financial interests.

ACKNOWLEDGMENT

This work was supported in part by JSPS KAKENHI Grants JP20H02730 (S.M.), JP20K15946 (M.K.), JP22K15239 (M.K.), JP20H05217 (M.G.) and JP20H02685 (J.H.). We thank Dr. Satoshi Maeda and Dr. Kimichi Suzuki at Hokkaido University for their support with computational studies using GRRM. We thank Dr. Mikako Ogawa and Dr. Hideo Takakura at Hokkaido University for their support in the determination of the quantum yield. This work was partly supported by Hokkaido University, Global Facility Center (GFC), Pharma Science Open Unit (PSOU), funded by MEXT under "Support Program for Implementation of New Equipment Sharing System." M.G. and J.H. appreciate Photoexcitonix project of Hokkaido University. Part of the calculations was performed at the Research Center for Computational Science, Okazaki, Japan (Project: 22-IMS-C172, 21-IMS-C168, 22-IMS-C002). This work was partly achieved through the use of the supercomputer system at the information initiative center of Hokkaido University.

REFERENCES

(1) (a) Hammond, G. S.; Turro, N. J., Organic Photochemistry. *Science* **1963**, *142*, 1541-1553. (b) Hoffmann, N., Photochemical Reactions as Key Steps in Organic Synthesis. *Chem. Rev.* **2008**, *108*, 1052-1103.

(2) For selected reviews, see: (a) Strieth-Kalthoff, F.; James, M. J.; Teders, M.; Pitzer, L.; Glorius, F., Energy transfer catalysis mediated by visible light: principles, applications, directions. *Chem. Soc. Rev.* **2018**, *47*, 7190-7202. (b) Zhou, Q.-Q.; Zou, Y.-Q.; Lu, L.-Q.; Xiao, W.-J., Visible-Light-Induced Organic Photochemical Reactions through Energy-Transfer Pathways. *Angew. Chem., Int. Ed.* **2019**, *58*, 1586-1604. (c) Strieth-Kalthoff, F.; Glorius, F., Triplet Energy Transfer Photocatalysis: Unlocking the Next Level. *Chem* **2020**, *6*, 1888-1903.

(3) For selected examples, see: (a) Heitz, D. R.; Tellis, J. C.; Molander, G. A., Photochemical Nickel-Catalyzed C–H Arylation: Synthetic Scope and Mechanistic Investigations. *J. Am. Chem. Soc.* **2016**, *138*, 12715-12718. (b) Welin, E. R.; Le, C.; Arias-Rotondo, D. M.; McCusker, J. K.; MacMillan, D. W. C., Photosensitized, energy transfer-mediated organometallic catalysis through electronically excited nickel(II). *Science* **2017**, *355*, 380-385. (c) Kudisch, M.; Lim, C.-H.; Thordarson, P.; Miyake, G. M., Energy Transfer to Ni-Amine Complexes in Dual Catalytic, Light-Driven C–N Cross-Coupling Reactions. *J. Am. Chem. Soc.* **2019**, *141*, 19479-19486. (d) Kim, T.; McCarver, S. J.; Lee, C.; MacMillan, D. W. C. Sulfonamidation of Aryl and Heteroaryl Halides through Photosensitized Nickel Catalysis. *Angew. Chem., Int. Ed.* **2018**, *57*, 3488-3492. € Lu, J.; Pattengale, B.; Liu, Q.; Yang, S.; Shi, W.; Li, S.; Huang, J.; Zhang, J. Donor–Acceptor Fluorophores for Energy-Transfer-Mediated Photocatalysis. *J. Am. Chem. Soc.* **2018**, *140*, 13719-13725. (f) Tian, L.; Till, N. A.; Kudisch, B.; MacMillan, D. W. C.; Scholes, G. D. Transient Absorption Spectroscopy Offers Mechanistic Insights for an Iridium/Nickel-Catalyzed C–O Coupling. *J. Am. Chem. Soc.* **2020**, *142*, 4555-4559. (g) Kancherla, R.; Muralirajan, K.; Maity, B.; Karuthedath, S.; Kumar, G. S.; Laquai, F.; Cavallo, L.; Rueping, M. Mechanistic insights into photochemical nickel-catalyzed cross-couplings enabled by energy transfer. *Nat. Commun.* **2022**, *13*, 2737.

(4) Zhang, Z.; Rogers, C. R.; Weiss, E. A., Energy Transfer from CdS QDs to a Photogenerated Pd Complex Enhances the Rate and Selectivity of a Pd-Photocatalyzed Heck Reaction. *J. Am. Chem. Soc.* **2020**, *142*, 495-501.

(5) Xia, Z.; Corcé, V.; Zhao, F.; Przybylski, C.; Espagne, A.; Jullien, L.; Le Saux, T.; Gimbert, Y.; Dossmann, H.; Mouriès-Mansuy, V.; Ollivier, C.; Fensterbank, L. Photosensitized oxidative addition to gold(I) enables alkynylative cyclization of *o*-alkylnylphenols with iodoalkynes. *Nat. Chem.* **2019**, *11*, 797-805.

(6) For an example of photosensitization of a copper amide complex, see: Yoo, W.-J.; Tsukamoto, T.; Kobayashi, S., Visible Light-Mediated Ullmann-Type C–N Coupling Reactions of Carbazole Derivatives and Aryl Iodides. *Org. Lett.* **2015**, *17*, 3640-3642.

(7) Photoinduced reduction of a rhodacycle intermediate might occur partly via photosensitization. See: Tanaka, J.; Nagashima, Y.; Araujo Dias, A. J.; Tanaka, K., Photo-Induced ortho-C–H Borylation of Arenes through In Situ Generation of Rhodium(II) Ate Complexes. *J. Am. Chem. Soc.* **2021**, *143*, 11325-11331.

(8) For selected reviews, see: (a) Bolm, C.; Legros, J.; Le Paih, J.; Zani, L., Iron-Catalyzed Reactions in Organic Synthesis. *Chem. Rev.* **2004**, *104*, 6217-6254. (b) *Iron Catalysis in Organic Chemistry: Reactions and Applications*; Plietker, B., Ed.; Wiley-VCH: Weinheim, Germany, 2008; pp 1-279. (c) Sun, C.-L.; Li, B.-J.; Shi, Z.-J. Direct C−H Transformation via Iron Catalysis. *Chem. Rev.* **2011**, *111*, 1293-1314. (d) Greenhalgh, M. D.; Jones, A. S.; Thomas, S. P. Iron-Catalysed Hydrofunctionalisation of Alkenes and Alkynes. *ChemCatChem* **2015**, *7*, 190-222. (e) Bauer, I.; Knölker, H.-J., Iron Catalysis in Organic Synthesis. *Chem. Rev.* **2015**, *115*, 3170-3387. (f) Fürstner, A., Iron Catalysis in Organic Synthesis: A Critical Assessment of What It Takes to Make This Base Metal a Multitasking Champion. *ACS Cent. Sci.* **2016**, *2*, 778-789. (g) Shang, R.; Ilies, L.; Nakamura, E., Iron-Catalyzed C–H Bond Activation. *Chem. Rev.* **2017**, *117*, 9086-9139. (h) Wei, D.; Darcel, C., Iron Catalysis in Reduction and Hydrometalation Reactions. *Chem. Rev.* **2019**, *119*, 2550-2610. (i) Gandeepan, P.; Müller, T.; Zell, D.; Cera, G.; Warratz, S.; Ackermann,

L., 3d Transition Metals for C–H Activation. *Chem. Rev.* **2019**, *119*, 2192-2452. (j) Arevalo, R.; Chirik, P. J., Enabling Two-Electron Pathways with Iron and Cobalt: From Ligand Design to Catalytic Applications. *J. Am. Chem. Soc.* **2019**, *141*, 9106-9123. For selected examples, see: (k) Lipschutz, M. I.; Chantarojsiri, T.; Dong, Y.; Tilley, T. D. Synthesis, Characterization, and Alkyne Trimerization Catalysis of a Heteroleptic Two-Coordinate Fe^{I} Complex. *J. Am. Chem. Soc.* **2015**, *137*, 6366-6372. (l) Sun, Y.; Tang, H.; Chen, K.; Hu, L.; Yao, J.; Shaik, S.; Chen, H. Two-State Reactivity in Low-Valent Iron-Mediated C–H Activation and the Implications for Other First-Row Transition Metals. *J. Am. Chem. Soc.* **2016**, *138*, 3715-3730. (m) Sharma, A. K.; Sameera, W. M. C.; Jin, M.; Adak, L.; Okuzono, C.; Iwamoto, T.; Kato, M.; Nakamura, M.; Morokuma, K. DFT and AFIR Study on the Mechanism and the Origin of Enantioselectivity in Iron-Catalyzed Cross-Coupling Reactions. *J. Am. Chem. Soc.* **2017**, *139*, 16117-16125. (n) Kimura, N.; Kochi, T.; Kakiuchi, F. Iron-Catalyzed Regioselective Anti-Markovnikov Addition of C–H Bonds in Aromatic Ketones to Alkenes. *J. Am. Chem. Soc.* **2017**, *139*, 14849-14852. (o) Lo, J. C.; Kim, D.; Pan, C.-M.; Edwards, J. T.; Yabe, Y.; Gui, J.; Qin, T.; Gutiérrez, S.; Giacoboni, J.; Smith, M. W.; Holland, P. L.; Baran, P. S. Fe-Catalyzed C–C Bond Construction from Olefins via Radicals. *J. Am. Chem. Soc.* **2017**, *139*, 2484-2503. (p) Braconi, E.; Götzinger, A. C.; Cramer, N., Enantioselective Iron-Catalyzed Cross-[4+4]-Cycloaddition of 1,3-Dienes Provides Chiral Cyclooctadienes. *J. Am. Chem. Soc.* **2020**, *142*, 19819-19824. (q) Liu, L.; Aguilera, M. C.; Lee, W.; Youshaw, C. R.; Neidig, M. L.; Gutierrez, O. General method for iron-catalyzed multicomponent radical cascades–cross-couplings. *Science* **2021**, *374*, 432-439. (r) Zhang, H.; Wang, E.; Geng, S.; Liu, Z.; He, Y.; Peng, Q.; Fang, Z. Experimental and Computational Studies of the Iron-Catalyzed Selective and Controllable Defluorosilylation of Unactivated Aliphatic *gem*-Difluoroalkenes. *Angew. Chem., Int. Ed.* **2021**, *60*, 10211-10218.

(9) Neumeier, M.; Chakraborty, U.; Schaarschmidt, D.; de la Pena O'Shea, V.; Perez-Ruiz, R.; Jacobi von Wangelin, A., Combined Photoredox and Iron Catalysis for the Cyclotrimerization of Alkynes. *Angew. Chem., Int. Ed.* **2020**, *59*, 13473-13478.

(10) Brenna, D.; Villa, M.; Gieshoff, T. N.; Fischer, F.; Hapke, M.; Jacobi von Wangelin, A., Iron-Catalyzed Cyclotrimerization of Terminal Alkynes by Dual Catalyst Activation in the Absence of Reductants. *Angew. Chem., Int. Ed.* **2017**, *56*, 8451-8454.

(11) For selected examples of Fe/photoredox dual catalysis, see: (a) Rao, H.; Schmidt, L. C.; Bonin, J.; Robert, M., Visible-light-driven methane formation from CO_2 with a molecular iron catalyst. *Nature* **2017**, *548*, 74-77. (b) Rao, H.; Lim, C.-H.; Bonin, J.; Miyake, G. M.; Robert, M. Visible-Light-Driven Conversion of CO_2 to CH_4 with an Organic Sensitizer and an Iron Porphyrin Catalyst. *J. Am. Chem. Soc.* **2018**, *140*, 17830-17834. (c) Ouyang, X.-H.; Li, Y.; Song, R.-J.; Hu, M.; Luo, S.; Li, J.-H., Intermolecular dialkylation of alkenes with two distinct C(sp^3)–H bonds enabled by synergistic photoredox catalysis and iron catalysis. *Sci. Adv.* **2019**, *5*, eaav9839. (d) Ning, Y.; Wang, S.; Li, M.; Han, J.; Zhu, C.; Xie, J. Site-specific Umpolung amidation of carboxylic acids via triplet synergistic catalysis. *Nat. Commun.* **2021**, *12*, 4637. (e) Neogi, S.; Kumar Ghosh, A.; Mandal, S.; Ghosh, D.; Ghosh, S.; Hajra, A. Three-Component Carbosilylation of Alkenes by Merging Iron and Visible-Light Photocatalysis. *Org. Lett.* **2021**, *23*, 6510-6514.

(12) For selected reviews of pyridine synthesis via metal-catalyzed [2+2+2] cycloaddition, see: (a) Vollhardt, K. P. C., Cobalt-Mediated [2 + 2 + 2]-Cycloadditions: A Maturing Synthetic Strategy [New Synthetic Methods (43)]. *Angew. Chem., Int. Ed. Engl.* **1984**, *23*, 539-556. (b) Heller, B.; Hapke, M. The fascinating construction of pyridine ring systems by transition metal-catalysed [2 + 2 + 2] cycloaddition reactions. *Chem. Soc. Rev.* **2007**, *36*, 1085-1094. For selected examples, see: (c) Wakatsuki, Y.; Yamazaki, H., Novel synthesis of heterocyclic compounds from acetylenes. *J. Chem. Soc., Chem. Commun.* **1973**, 280a. (d) Vollhardt, K. P. C.; Bergman, R. G., One-step synthesis of benzocyclobutenes involving cooligomerization of linear mono- and diacetylenes catalyzed by η^5-cyclopentadienylcobalt dicarbonyl. *J. Am. Chem. Soc.* **1974**, *96*, 4996-4998. (e) Yamamoto, Y.; Kinpara, K.; Saigoku, T.; Takagishi, H.; Okuda, S.; Nishiyama, H.; Itoh, K. Cp*RuCl-Catalyzed [2 + 2 + 2] Cycloadditions of α,ω-Diynes with Electron-Deficient Carbon−Heteroatom Multiple Bonds Leading to Heterocycles. *J. Am. Chem. Soc.* **2005,** *127*, 605-613. (f) Tanaka, K.; Suzuki, N.; Nishida, G., Cationic Rhodium(I)/Modified-BINAP Catalyzed [2+2+2] Cycloaddition of Alkynes with Nitriles. *Eur. J. Org. Chem.* **2006**, 3917-3922. (g) Onodera, G.; Shimizu, Y.; Kimura, J.-n.; Kobayashi, J.; Ebihara, Y.; Kondo, K.; Sakata, K.; Takeuchi, R. Iridium-Catalyzed [2 + 2 + 2] Cycloaddition of α,ω-Diynes with Nitriles. *J. Am. Chem. Soc.* **2012**, *134*, 10515-10531. (h) Tan, J.-F.; Bormann, C. T.; Perrin, F. G.; Chadwick, F. M.; Severin, K.; Cramer, N. Divergent Synthesis of Densely Substituted Arenes and Pyridines via Cyclotrimerization Reactions of Alkynyl Triazenes. *J. Am. Chem. Soc.* **2019**, *141*, 10372-10383. (i) Wang, C.-S.; Sun, Q.; García, F.; Wang, C.; Yoshikai, N. Robust Cobalt Catalyst for Nitrile/Alkyne [2+2+2] Cycloaddition: Synthesis of Polyarylpyridines and Their Mechanochemical Cyclodehydrogenation to Nitrogen-Containing Polyaromatics. *Angew. Chem.*, *Int. Ed.* **2021**, *60*, 9627-9634.

(13) For selected examples, see: (a) Knoch, F.; Kremer, F.; Schmidt, U.; Zenneck, U.; Le Floch, P.; Mathey, F. (η^4-1,5-Cyclooctadiene)(η^6-phosphinine)iron(0): Novel Room-Temperature Catalyst for Pyridine Formation. *Organometallics* **1996**, *15*, 2713-2719. (b) Ferré, K.; Toupet, L.; Guerchais, V. Alkyne Coupling Reactions Mediated by Iron(II) Complexes: Highly Chemo- and Regioselective Formation of η^6-Coordinated Arene and Pyridine Complexes. *Organometallics* **2002**, *21*, 2578-2580. (c) Richard, V.; Ipouck, M.; Mérel, D. S.; Gaillard, S.; Whitby, R. J.; Witulski, B.; Renaud, J.-L. Iron(II)-catalysed [2+2+2] cycloaddition for pyridine ring construction. *Chem. Commun.* **2014**, *50*, 593-595. (d) Casitas, A.; Krause, H.; Goddard, R.; Fürstner, A. Elementary Steps of Iron Catalysis: Exploring the Links between Iron Alkyl and Iron Olefin Complexes for their Relevance in C–H Activation and C–C Bond Formation. *Angew. Chem.*, *Int. Ed.* **2015**, *54*, 1521-1526.

(14) For selected examples, see: (a) Wang, C.; Li, X.; Wu, F.; Wan, B. A Simple and Highly Efficient Iron Catalyst for a [2+2+2] Cycloaddition to Form Pyridines. *Angew. Chem.*, *Int. Ed.* **2011**, *50*, 7162-7166. (b) Harper, J. L.; Felten, S.; Stolley, R. M.; Hegg, A. S.; Cheong, P. H. Y.; Louie, J. Origins of Regio- and Chemoselectivity in Iron-PDAI-Catalyzed [2+2+2] Cycloaddition Syntheses of 4,6-Disubstituted 2-Aminopyridines. *ACS Catal.* **2021**, *11*, 14677-14687.

(15) For discussion regarding the beneficial effect of iodide, see section 6-1-5 of Supporting Information.

(16) For selected catalytic reactions facilitated by combination of low-valent first-row metals and dppp, see: (a) Lin, X.; Zheng, F.; Qing, F.-L. Iron-Catalyzed Cross-Coupling Reactions between Arylzinc Reagents and Alkyl Halides Bearing β-Fluorines. *Organometallics* **2011**, *31*, 1578-1582. (b) Thullen, S. M.; Rovis, T. A Mild Hydroaminoalkylation of Conjugated Dienes Using a Unified Cobalt and Photoredox Catalytic System. *J. Am. Chem. Soc.* **2017**, *139*, 15504-15508. (c) Wu, C.; Yoshikai, N. Cobalt-Catalyzed Intramolecular Reactions between a Vinylcyclopropane and an Alkyne: Switchable [5+2] Cycloaddition and Homo-Ene Pathways. *Angew. Chem., Int. Ed.* **2018**, *57*, 6558-6562. See also 14a.

(17) (a) Low, K.-H.; Dai, L.; Chen, J.; Cai, L. ORGANIC ELECTROLUMINESCENT MATERIAL AND ORGANIC ELECTROLUMINESCENT DEVICE. US20160260907A1, **2016**. (b) Chen, X.; Lu, P.; Wang, Y., Four Iodine-Mediated Electrophilic Cyclizations of Rigid Parallel Triple Bonds Mapped from 1,8-Dialkynylnaphthalenes. *Chem. – Eur. J.* **2011**, *17*, 8105-8114. (c) Pal, S.; Metin, Ö.; Türkmen, Y. E. Synthesis of Fluoranthene Derivatives via Tandem Suzuki–Miyaura and Intramolecular C–H Arylation Reactions under Both Homogeneous and Heterogeneous Catalytic Conditions. *ACS Omega* **2017**, *2*, 8689-8696. (d) Dong, P.; Majeed, K.; Wang, L.; Guo, Z.; Zhou, F.; Zhang, Q., Transition metal-free approach to azafluoranthene scaffolds by aldol condensation/[1+2+3] annulation tandem reaction of isocyanoacetates with 8-(alkynyl)-1-naphthaldehydes. *Chem. Commun.* **2021**, *57*, 4855-4858.

(18) For highly crystalline azafluoranthenes (**5ba**, **5da**), the products were obtained in higher yield when the reaction was performed at a lower concentration using two blue LED panels (See Supporting Information for detailed reaction setup).

(19) UV-vis spectra of some new azafluoranthenes in solution and photoluminescence of **5da** at 365 nm in the solid state are provided in section 5 of Supporting Information.

(20) The cycloaddition proceeded in synthetically useful yield (**4aa**: 62%, **5aa**: 65%) when the amount of nitrile was reduced to 1.5 equivalents. For details, see section 2-3 of Supporting Information.

(21) For an attempt of fully intermolecular [2+2+2] cycloaddition, see section 2-4 of Supporting Information.

(22) The reaction in the dark under mild heating did not result in the improvement of the yield of **4fa**, indicating that the acceleration effect is more likely to be derived from light than the heat from LED. See section 4-3 of Supporting Information for details.

(23) The authors have unexpectedly discovered that, in the reaction in **Scheme 3A, (iii)**, **4fa** was obtained in varying yield after several trials (lowest: 5%, highest: 30%). Although the exact cause of the limited repeatability is not clear at present, the reaction was repeated for 7 times with our best efforts in the purity of materials and precision in reaction setups, and the average of the thus obtained 7 results was employed for a fair comparison. The same consideration was made in the reactions in **Scheme 3B, (v)** and **Scheme 3B, (vi)**. See section 4-3 of Supporting Information for details.

(24) For selected examples of reactions mediated by direct photoexcitation of an iron complex, see: (a) Wei, X.-J.; Abdiaj, I.; Sambiagio, C.; Li, C.; Zysman-Colman, E.; Alcázar, J.; Noël, T., Visible-Light-Promoted Iron-Catalyzed $C(sp^2)$–$C(sp^3)$ Kumada Cross-Coupling in Flow. *Angew. Chem.*, *Int. Ed.* **2019**, *58*, 13030-13034. (b) Kang, Y. C.; Treacy, S. M.; Rovis, T. Iron-Catalyzed Photoinduced LMCT: A 1° C–H Abstraction Enables Skeletal Rearrangements and $C(sp^3)$–H Alkylation. *ACS Catal.* **2021**, *11*, 7442-7449. (c) Tang, J.-J.; Yu, X.; Wang, Y.; Yamamoto, Y.; Bao, M. Interweaving Visible-Light and Iron Catalysis for Nitrene Formation and Transformation with Dioxazolones. *Angew. Chem.*, *Int. Ed.* **2021**, *60*, 16426-16435. (d) Xue, T.; Zhang, Z.; Zeng, R. Photoinduced Ligand-to-Metal Charge Transfer (LMCT) of Fe Alkoxide Enabled C–C Bond Cleavage and Amination of Unstrained Cyclic Alcohols. *Org. Lett.* **2022**, *24*, 977-982. (e) Hou, M.; Zhang, Z.; Lai, X.; Zong, Q.; Jiang, X.; Guan, M.; Qi, R.; Qiu, G. Photoredox/Iron Dual-Catalyzed Insertion of Acyl Nitrenes into C–H Bonds. *Org. Lett.* **2022**, *24*, 4114-4118.

(25) See section 6-1 of Supporting Information for more details of DFT calculations.

(26) Messinis, A. M.; Luckham, S. L. J.; Wells, P. P.; Gianolio, D.; Gibson, E. K.; O'Brien, H. M.; Sparkes, H. A.; Davis, S. A.; Callison, J.; Elorriaga, D.; Hernandez-Fajardo, O.; Bedford, R. B. The highly surprising behaviour of diphosphine ligands in iron-catalysed Negishi cross-coupling. *Nat. Catal.* **2019**, *2*, 123-133.

(27) (a) Nakatsuji, N. Cluster expansion of the wavefunction. Excited states. *Chem. Phys. Lett.* **1978**, *59*, 362-364. (b) Nakatsuji, H. Description of Two- and Many-Electron Processes by the SAC-CI Method. *Chem. Phys. Lett.* **1991**, *177*, 331-337.

(28) Speckmeier, E.; Fischer, T. G.; Zeitler, K. A Toolbox Approach To Construct Broadly Applicable Metal-Free Catalysts for Photoredox Chemistry: Deliberate Tuning of Redox Potentials and Importance of Halogens in Donor−Acceptor Cyanoarenes. *J. Am. Chem. Soc.* **2018**, *140*, 15353-15365.

(29) See section 4-5 of Supporting Information for details of the determination of Φ. While $\Phi < 1$ does not strictly exclude the involvement of catalytic cycle in the dark, $\Phi > 1$ is characteristic of reactions in which photochemical initiation followed by catalytic turnover in the absence of photonic input is a dominant reaction pathway. For selected mechanistic studies of photoreactions with $\Phi > 1$, see: (a) Cismesia, M. A.; Yoon, T. P. Characterizing chain processes in visible light photoredox catalysis. *Chem. Sci.* **2015**, *6*, 5426-5434. (b) Till, N. A.; Tian, L.; Dong, Z.; Scholes, G. D.; MacMillan, D. W. C. Mechanistic Analysis of Metallaphotoredox C–N Coupling: Photocatalysis Initiates and Perpetuates Ni(I)/Ni(III) Coupling Activity. *J. Am. Chem. Soc.* **2020**, *142*, 15830-15841.

(30) For experimental details of the light/dark experiment, see section 4-6 of Supporting Information. When $\Phi < 1$ due to low efficiency in photoinitiation but following dark catalytic turnover renders a significant contribution to the product formation, the yield in entry 2 is expected to be higher than that of entry 1.

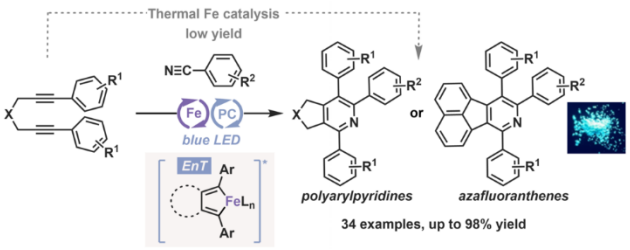
Thermal Fe catalysis
low yield
Fe
PC
blue LED
EnT
Ar
FeLn
Ar
polyarylpyridines
or
azafluoranthenes
34 examples, up to 98% yield